



# Green Synthesis of Highly Dispersed Zinc Oxide Nanoparticles Supported on Silica Gel Matrix by *Daphne oleoides* Extract and their Antibacterial Activity

Laleh Safavinia<sup>1</sup>, Mohammad Reza Akhgar<sup>1\*</sup>, Batool Tahamipour<sup>2</sup>, Sayed Ali Ahmadi<sup>1</sup>

<sup>1</sup>Department of Chemistry, Faculty of Science, Kerman Branch, Islamic Azad University, Kerman, Iran

<sup>2</sup>Young Researchers and Elite Club, Sirjan Branch, Islamic Azad University, Sirjan, Iran

\*Corresponding author: Mohammad Reza Akhgar, Department of Chemistry, Faculty of Science, Kerman Branch, Islamic Azad University, Kerman, Iran; Tel/Fax: +98-3431321338; E-mail: akhgar@iauk.ac.ir

**Background:** ZnO nanoparticles (ZnO-NPs) are one of the most popular metal oxide nanoparticles, which exhibit significant antibacterial properties against various pathogens. Among nanoparticle synthesis methods, the green synthesis using plant extract is considered as an eco-friendly and cost-effective method for ZnO-NPs production, compared to the chemical procedures.

**Background:** This study aimed to evaluate the green synthesis of ZnO-NPs loaded on silica gel matrix (ZnO/SG nanocomposite) by using methanol leaf extract of *Daphne oleoides* as a new extract and a cost-effective method. Furthermore, the antibacterial activity of the synthesized structure is evaluated against some pathogenic bacteria and the results are compared with unsupported ZnO-NPs.

**Materials and Methods:** For ZnO/SG nanocomposite synthesis, a solution of Zn (NO<sub>3</sub>)<sub>2</sub> was stirred with silica gel. Then the *Daphne oleoides* extract was added and stirred continuously until white precipitate was formed. The precipitate was heated at 200 °C for calcination, and ZnO/SG nanocomposite was obtained. The phytochemical constituents of leaf extract were then analyzed by gas chromatography–mass spectrometry (GC-MS). Afterwards, the structure of ZnO-NPs on SiO<sub>2</sub> matrix (ZnO/SG nanocomposite) was characterized by field emission scanning electron microscopy (FESEM), energy-dispersive X-ray spectroscopy (EDS), X-ray diffraction analysis (XRD), and Fourier transform infrared spectroscopy (FTIR). Surface area measurement was also determined by Brunauer-Emmett-Teller (BET) techniques. Furthermore, the antibacterial activity of ZnO/SG nanocomposites against pathogenic bacteria was evaluated using agar-based disk diffusion method standardized by clinical and laboratory guidelines.

**Results:** The leaf extract of *Daphne oleoides* encompassed five major polyphenolic components. The results of the nanocomposite structure showed that ZnO-NPs with an average particle size of 38 nm were obtained and stabilized on the silica gel matrix. The BET surface area measurement of ZnO/SG nanocomposite was compared with unsupported ZnO-NPs, and the results indicated that the surface area of ZnO/SG nanocomposite was increased. Furthermore, the structure showed more powerful antibacterial activity against pathogens than unsupported ZnO-NPs.

**Conclusions:** Green synthesis of ZnO-NPs supported on the silica gel matrix with the leaf extract of *Daphne oleoides* is a benign and effective procedure for ZnO/SG nanocomposite synthesis. Embedding ZnO-NPs in silica gel matrix prevents the agglomeration of nanoparticles and prepare homodispersed nanoparticles. This structure revealed great antibacterial activity against many pathogens.

**Keywords:** Antibacterial Activity, *Daphne oleoides* extract, Green chemistry, ZnO Nanoparticles, Silica gel

## 1. Background

Nowadays, infectious diseases induced by various pathogenic microbes are widespread as a serious problem worldwide. Although numerous antimicrobial agents have been developed to kill or inhibit bacteria, the treatment of many infectious diseases is still a challenge.

Accordingly, industrial demands for materials with effective antibacterial properties are highly desirable. Nanotechnology has branched out in a large number of different fields of sciences, especially biology and medicine, because of its large-scale applications (1-3). Nanomaterials possess unique physical and chemical

**Copyright** © 2021 The Author(s); Published by National Institute of Genetic Engineering and Biotechnology. This is an open access article, distributed under the terms of the Creative Commons Attribution-NonCommercial 4.0 International License (<http://creativecommons.org/licenses/by-nc/4.0/>) which permits others to copy and redistribute material just in noncommercial usages, provided the original work is properly cited.

properties, compared to bulk counterparts, due to their high surface area and nanoscale size (4, 5). Metal oxide nanoparticles are a large group of nanomaterials, which have attracted the attention of the research community due to their special chemical and biological properties (6). The particular properties of the metal oxide nanoparticles have been exploited in various industrial applications such as food, agriculture, cosmetics, and medical field (7-10).

Among different metal oxide nanoparticles, zinc oxide nanoparticles (ZnO-NPs) are of great importance due to their unique properties. They have remarkable antimicrobial properties against various pathogens; therefore, they have great potentials to be used in food, biological, and medical industries (11). Furthermore, due to low cytotoxic effects in the environment, ZnO-NPs can be used as an effective antimicrobial agent against some bacterial pathogens in animals and fish (12).

The agglomeration of nanoparticles is a serious problem for unsupported ZnO-NPs during the synthesis process, which reduces its surface area and may alter the physiochemical properties, reactivity and morphology of the nanoparticles (13). In order to overcome this problem and enhance its dispersion, loading the ZnO nanoparticles on inert materials with high surface support, including silica gel matrix, is suggested (14). Silica gel provides a structural basis for many industrial applications as it is porous, biocompatible, and hydrothermally stable (15). Loading ZnO-NPs on silica gel matrix maintain the size and properties of ZnO-NPs unchanged during their reaction because the nanoparticles are trapped into an inert solid matrix (16). ZnO nanoparticles have been synthesized by different chemical methods such as co-precipitation, hydrothermal, solvothermal and chemical vapor deposition (17, 18). Since the chemical procedures have negative effects on the environment, there is a growing necessity to develop environmentally benign and eco-friendly methods not using toxic materials in the nanoparticle synthesis procedures (19). The green synthesis of nanoparticles using plant extracts is gaining greater importance due to its simplicity, cost-effectiveness, safety, and biocompatibility, compared to the chemical synthesis methods. Furthermore, nanoparticles produced by plant extracts are more stable and more varied in shape and size, in comparison to the ones produced by other methods (20-22)

Recently, various plant extracts such as tea leaf (23), fruit peel (24), tomato (*Lycopersicon esculentum*) (25), and Eucalyptus (26) and some native plant extracts (27, 28) have acted as eco-friendly precursors for the

synthesis of ZnO-NPs and have potential applications. Among native plant extracts, Iranian native plants have attracted the attention of researchers in the field of nanoparticle synthesis because of their interesting chemical components. Nevertheless, Iran is a broad country and rich in native plants with a variety of special plant species, many of which have not been adequately explored.

The genus *Daphne* belonging to the Thymelaeaceae family is often found on calcareous rocks and rocky slopes at altitudes above 2000 m. Many species of the genus have been of great interest owing to their excellent medicinal and chemical values. The extract of several *Daphne* species is used as an antibacterial, antileukemic, and antioxidant agent in biomedical applications or wound healing processes (29).

This study describes the green synthesis of ZnO nanoparticles loaded on silica gel matrix with *Daphne oleoides* leaf extract as a new extract.

## 2. Objectives

The primary objective of the present study was to evaluate the green synthesis of ZnO nanoparticles supported on silica gel matrix using *Daphne oleoides* methanol leaf extract as a new and beneficial platform for the production of ZnO/SG nanocomposites. In this study, we reported the phytochemical analysis of *Daphne oleoides* species found in Hezar Mountains of Kerman, Iran. Furthermore, the antibacterial activity of ZnO/SG nanocomposites against some pathogenic bacteria, especially in fish pathogens, has been evaluated.

## 3. Materials and Methods

### 3.1. Materials

Zinc nitrate hexahydrate ( $Zn(NO_3)_2 \cdot 6H_2O$ ), silica gel (particle size 63-200  $\mu m$ ), methanol (HPLC grade >99.8%), formic acid (HPLC grade >98 %), and all the other chemicals were purchased from Sigma Aldrich and used without further purification.

The bacterial strains used for the antibacterial activity was bacterial fish such as *Edwardsiella tarda* (IBRC-M 10718) and *Loctococcus garvieae* (IBRC-M 10900), gram-positive bacterial strains such as *Bacillus cereus* (PTCC 1665) and *Staphylococcus epidermidis* (PTCC 1435), and Gram-negative bacterial strains such as *Salmonella enterica* (PTCC 1709), *Klebsiella pneumoniae* (PTCC 1290), and *Escherichia coli* (PTCC 1399) were prepared from the Persian Type Culture Collection (PTCC) and Iranian Biological Resource Center (IBRC), Tehran, Iran.

To prepare *Daphne oleoides* extract, 50 g of dried and cleaning leaves was immersed in 250 mL of methanol and magnetically stirred for one h at 60 °C. The mixture was cooled down to room temperature and filtered by Whatman filter paper, followed by Millipore filter. The filtered extract was stored in a refrigerator at 4 °C for further studies.

### 3.2. Green Synthesis of Zinc Oxide Nanoparticles Supported on Silica Gel

First, 100 mL of Zn (NO<sub>3</sub>)<sub>2</sub> solution (0.5 M) in water was transferred to a 250 mL Erlenmeyer flask, and 3 g of silica gel was dispersed into solution via stirring. Then 20 mL of *Daphne oleoides* methanol extract was added slowly and stirred continuously during 30 min until white precipitate was formed. The precipitate was centrifuged at 10,000 x g for 5 min and washed twice with methanol and deionized water to remove impurities. Finally, the precipitate was heated in a muffle furnace at 200 °C for 4 h as such calcination and ZnO/SG nanocomposites were obtained.

### 3.3. Chemical Synthesis of Zinc Oxide Nanoparticles Supported on Silica Gel

ZnO/SG nanocomposites were prepared by precipitation method, as mentioned in relevant literature (14).

First, 2 gr SiO<sub>2</sub> and 10 mL zinc nitrate solution (0.5M) were poured in a beaker. Then 20 mL of NaOH solution (0.5M) was added dropwise to the slurry, and the mixture was stirred at 60 °C for 1 h. The precipitate was filtered, washed and calcined at 400 °C for 1 h to obtain ZnO/SG nanocomposites.

### 3.4. Characterization

The structure of ZnO/SG nanocomposite was characterized for their particle morphologies, elemental analysis, and crystal phases. The surface morphology was observed with a field emission scanning electron microscope (FESEM, model :Mira 3-TESCAN). The high resolution SEM images of the samples were quantitatively analyzed by Image J software (National Institutes of Health version 1.48v).

The elemental analysis was surveyed with an energy-dispersive X-ray spectroscopy (EDS model SAMx) at an accelerating voltage of 100 KV. The synthesized ZnO/SG nanocomposite crystallite size was identified by X'-Pert PRO (Philips, Model: PW3064) X-ray diffractometer. The further analysis of structural parameter of diffraction pattern was performed by the Highscore plus V3. X-ray diffraction Cu K<sub>α</sub> radiation (λ 1.54 Å) in 2θ range from 10 to 80. Fourier transform

infrared spectroscopy (FT-IR, Shemadzu) was also used to characterize the ZnO functional groups. The surface area measurement determined by Brunauer-Emmett-Teller (BET) techniques was performed on the analyzer ( BELSORP model: MINI II) to analyze the specific surface area of ZnO/SG nanocomposite, in comparison to unsupported ZnO nanoparticles. For phytochemical analysis of the extract by HPLC, the stock solution of the extract was freshly prepared at 5 mg.mL<sup>-1</sup> volume in methanol and then filtrated with a 0.45 μm syringe Whatman filter. The HPLC profiles of the extract were performed using Agilent Technologies 1200 series system (Germany) with a SPD20A prominence diode array detector (DAD), in the Research and Education Center for Agricultural and Natural Resources in Shiraz, Fars. The wavelength scanning was performed between 280 to 320 nm, and any wavelength was carefully monitored. Afterwards, 20 μL of each extract (300 μg.mL<sup>-1</sup>) was injected into the column Zorbax eclipse (XDB) C18, 5μm (ID), 4.6 × 150 mm (FT). Phytochemicals was conducted using the following mobile phase (methanol: formic acid 1%), and gradient/hold time was (10:90): 0 min, (25:75): 10 min, (60:40): 20 min, (70:30): 30 min, and (70:30): 40 min. The flow rate of the mobile phase varied in the range of 0.5–1.0 mL.min<sup>-1</sup>.

### 3.5. Antibacterial Activity

The antibacterial activity of ZnO/SG nanocomposites was studied by using agar-based disk diffusion assay standardized by the clinical and laboratory guidelines (30). For agar diffusion assay, the agar solution was uniformly spread on Petri dishes with a diameter of 80 mm, and a suspension of microorganism (5x10<sup>7</sup> CFUs) was sprayed across the whole area of each Petri dish. To prepare appropriate dispersions for bacterial killing, ZnO/SG nanocomposite powder was sonicated into distilled water for 3 min until a uniform colloidal suspension was formed. Then 1 mL of ZnO/SG nanocomposites with 10 mg.mL<sup>-1</sup> concentrations, as an antibacterial agent, was placed in a 2.5 mm well in the Petri dishes. The Petri dishes were incubated at 37 °C for 24 h at 90% humidity. The antibacterial activity was assessed by the width of an inhibition zone diameter (IZD) around the sample, and gentamicin (as antibacterial drug) was used as a controller. Moreover, antibacterial activities were compared by measuring the minimum inhibitory concentration (MIC) and minimum bactericidal concentration (MBC) of the sample. The experiment was repeated with unsupported ZnO nanoparticles to better compare the results.

## 4. Results

### 4.1. HPLC Fingerprint and Phytochemical Content of *Daphne Oleoides* Extract

The HPLC fingerprints at a wavelength of 280 nm were investigated for the *Daphne oleoides* extract. The concentrations of the components were determined by the percentage of the area in the peak in the HPLC fingerprints. **Table 1** shows five major compounds of the extract.

**Figure S1 (S1 (supplementary file))** presents the results of HPLC fingerprints, and 17 phytochemicals are indicated as retention time labeled-peaks. All of these phytochemicals are presented before the retention time of 30 minutes.

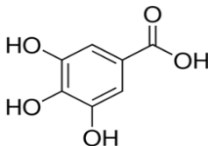
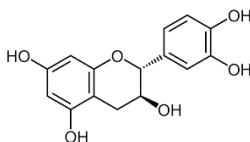
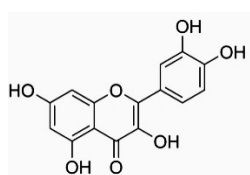
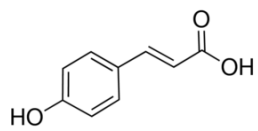
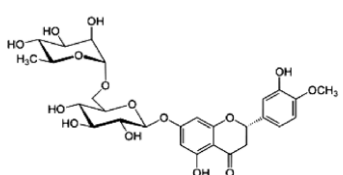
### 4.2. Characterization of ZnO/SG Nanocomposite

The precipitation of white suspension in the solution during green synthesis demonstrated the ZnO

nanoparticles synthesis. The morphological analysis of the green synthesized ZnO/SG nanocomposite was revealed by the SEM image. The ZnO nanoparticles synthesized in this study were 30-44 nm in size with spherical morphology (**Fig. 1**). The elemental analysis with energy-dispersive X-ray spectroscopy (EDS) showed three main peaks for Zn, O, and Si, thereby confirming ZnO/SG nanocomposite synthesis. The composition obtained from the EDX analysis contained zinc (11.33%), oxygen (72.02%), and silicon (16.65%). The minor peak in EDS graph was due to trace organic impurities in the sample (**Fig. 1**).

The XRD patterns of ZnO/SG nanocomposite are shown in **Figure 2** and compared with the XRD patterns of ZnO nanoparticles and silica gel. Diffraction peaks were observed at  $2\theta$  values of 32.99, 38.29, 45.26, 49.47, 55.31 and 65.97, corresponding to lattice planes (111), (200), (211), (102), (221) and (200), respectively. They were attributed to ZnO nanoparticles. These strong

**Table 1.** Content of phenolic compounds in methanol leaf extract of *Daphne oleoides*

Compound	Content (mg.L <sup>-1</sup> )	Retention time (min)	Structure
Gallic acid	2444.877	3.3	
Catechin	814.7272	8.3	
Quercetin	645.7424	21.6	
<i>p</i> -Coumaric acid	118.2411	15.6	
Hesperedin	1394.131	18.5	

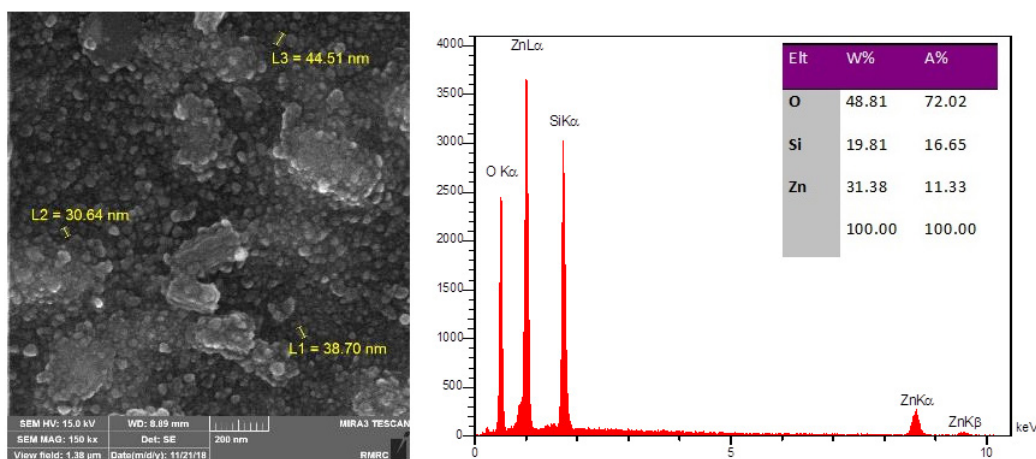


Figure 1. SEM images and EDX results of ZnO/SG nanocomposites

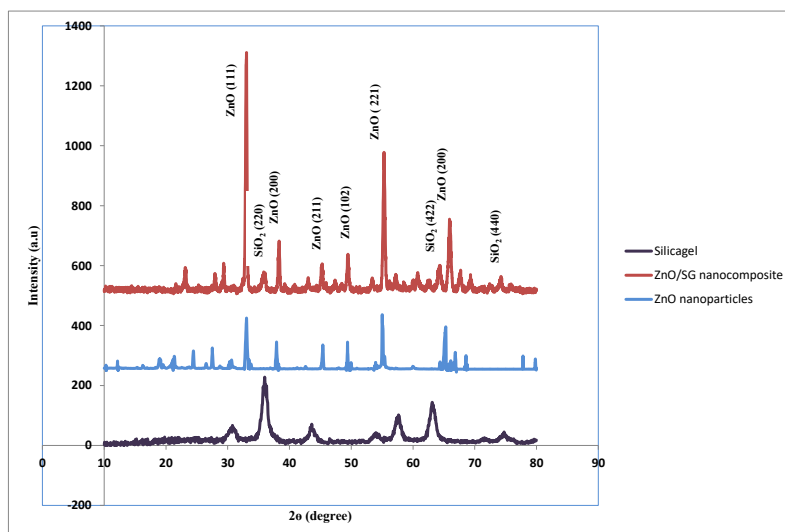


Figure 2. XRD patterns of ZnO/SG nanocomposite were recorded in the range of 20–80 of  $2\theta$  angles

peaks confirmed the ZnO nanoparticles stabilization in  $\text{SiO}_2$  matrix and approved the proposed structure.

The FTIR spectrum of ZnO/SG nanocomposite recorded in the range of 400–4000  $\text{cm}^{-1}$  is shown in **Figure S2**, supplementary file. The spectrum of this structure showed some broad peaks around 472, 1093, 1636 and 3439  $\text{cm}^{-1}$ , corresponding to chemical bonding between Zn-O and Si-O in ZnO/SG nanocomposites (31). The weak peaks at 1382 and 1636  $\text{cm}^{-1}$  for the minor organic compounds remained in ZnO/SG nanocomposite.

The BET surface area measurement for ZnO/SG nanocomposite in **Figure 3** exhibits type IV isotherms with specific surface areas ( $3.72 \times 10$  and  $24.5 \times 10 \text{ m}^2 \cdot \text{g}^{-1}$ ), total pore volume (0.2091 and  $0.5677 \text{ cm}^3 \cdot \text{g}^{-1}$ ), and mean pore diameter (22.47 and 9.25 nm) assigned to ZnO-NPs and ZnO/SG nanocomposites, respectively. Furthermore, the morphology and particle size

distribution of chemically synthesized ZnO/SG nanocomposite was revealed by the SEM image. The images showed that the ZnO nanoparticles were loaded uniformly on the surface of amorphous  $\text{SiO}_2$  with an average size of 45 nm (**Fig. S3**, supplementary file).

#### 4.3. Antibacterial Activity

The antibacterial activity of the ZnO/SG nanocomposites (1 mL of 10  $\text{mg} \cdot \text{mL}^{-1}$  concentrations) against two fish bacteria and some Gram-positive and Gram-negative bacteria is shown in **Table 2** and compared with that of the ZnO nanoparticles. These results show the width of the inhibition zone around different samples, which ranges from 8.79 mm for *Escherichia coli* to 13.62 mm for *Klebsiella pneumoniae*. Moreover, minimum inhibitory concentration (MIC) and minimum bactericidal concentration (MBC) for *Klebsiella*

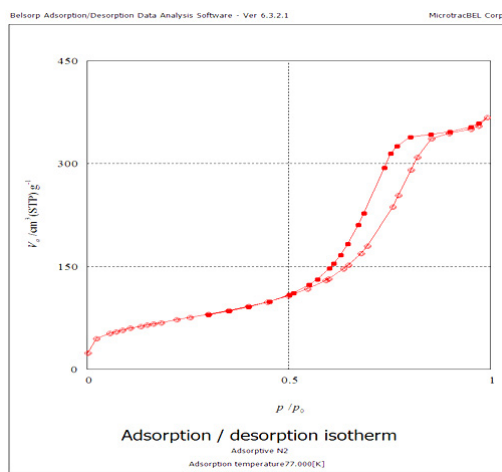


Figure 3. N2 adsorption/desorption isotherms for ZnO/SG nanocomposites

Table 2. Antibacterial activity of ZnO/SG nanocomposite compared to ZnO nanoparticles

	Bacteria		ZnO nanoparticles (mg.mL <sup>-1</sup> )	ZnO/SiO <sub>2</sub> nanocomposite (mg.mL <sup>-1</sup> )	Gentamicin(mg.mL <sup>-1</sup> )
Gram- positive	1665	IZD	9.42	12.27	23.82
		MIC	2048	512	1
		MBC	4096	1024	4
	1435	IZD	-	9.79	25.19
		MIC	-	2048	2
		MBC	-	4096	4
Gram- negative	1709	IZD	-	10.52	26.14
		MIC	-	1024	4
		MBC	-	2048	8
	1290	IZD	10.12	13.62	19.83
		MIC	1024	512	4
		MBC	2048	256	16
Fish bacterial	1399	IZD	4.5	8.79	24.26
		MIC	2048	1024	16
		MBC	4096	2048	16
	10718	IZD	-	11.75	15.98
		MIC	-	1024	4
		MBC	-	2048	2
10900	IZD	9.73	12.76	16.51	
	MIC	2048	1024	16	
	MBC	4096	2048	8	

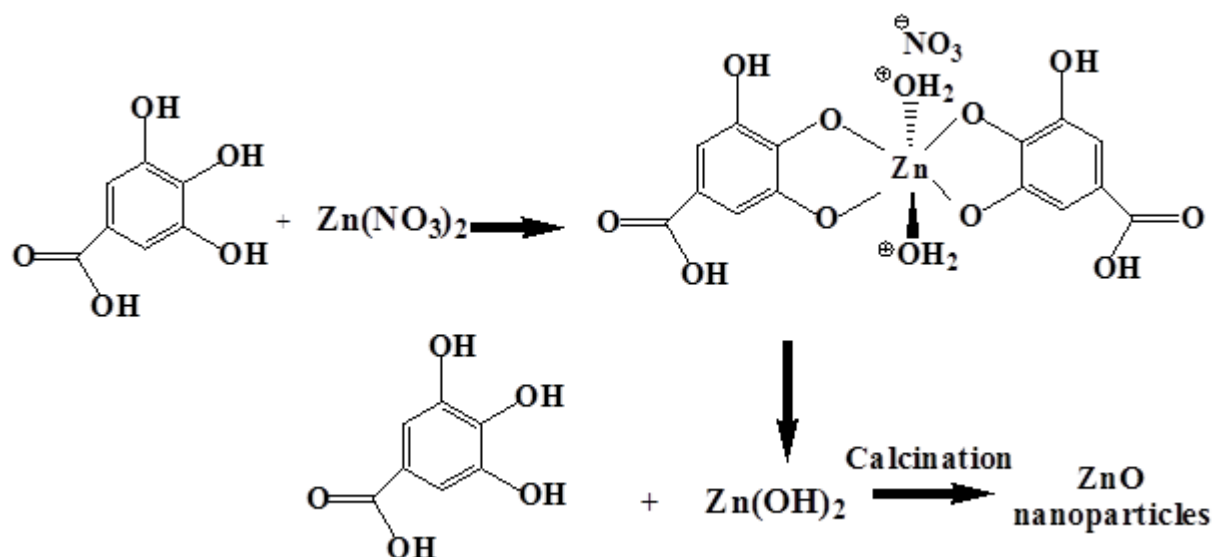
*pneumoniae* are 512 and 256 *pneumonia*, respectively.

The image of the antibacterial activity of the ZnO-NP and ZnO/SG nanocomposite and inhibition zone against *Klebsiella pneumoniae* (PTCC 1290) and *Loctococcus garvieae* (IBRC-M 10900) is shown in **Figure S4**, supplementary file

Furthermore, the antibacterial activity of the chemical and biosynthesized ZnO/SG against *Loctococcus garvieae* (IBRC-M 10900) was compared, and there was a similar inhibition zone in the range of 12.76 mm (**Fig. S5**, supplementary file).

## 5. Discussion

Nowadays numerous chemical methods have been developed for the synthesis of ZnO nanoparticles, which allow the production of particles with defined sizes and dimensions in many research areas. Chemical-based Zn-O nanoparticle synthesis requires the use of chemical-reducing agents and organic solvents. The major disadvantage of this chemical method is the use of highly deleterious chemical reagents, which are quite expensive and potentially hazardous to the environment. The green synthesis of ZnO nanoparticle with plant



**Scheme 1.** Plausible ZnO nanoparticle formation mechanism with phenolic compound in *Daphne oleoides* extract

extract has advantages in comparison to chemical methods since it is a cheap and fast method using low energy and a simple technique. Further, it is an eco-friendly method performed under ambient conditions and does not require large quantities of toxic chemicals. (32)

Accordingly, the green synthesis of ZnO nanoparticles has been proposed as an eco-friendly alternative to chemical synthetic methods.

In this study, we have employed *Daphne oleoides* methanol extract as a new and native plant extract in Iran to synthesize ZnO-NPs. This synthesis is usually done at ambient temperatures with neutral pH and benign fashion not using toxic materials.

Although many parts of this plant, including flowers, leaves and stems, can be used for extract production, we used fresh leaves of the plant for extract production. The HPLC analysis of the extract is rich in phytochemicals, especially polyphenolic compounds, such as Gallic acid, catechin, quercetin, *p*-coumaric acid and hesperedin (**Table 1**). These polyphenolic compounds act as both reduction and stabilization agents in ZnO-NPs synthesis.

**Scheme 1** shows the probable mechanism for the formation of zinc oxide nanoparticles. Polyphenolic compounds are the main constituents isolated from *Daphne oleoides*. Gallic acid has the highest concentration of polyphenolic component in the extract, and it seems to be responsible for the formation and stabilization of ZnO nanoparticles. When Gallic acid combines with zinc nitrate, it forms a Zn-OR complex via weak hydrogen bonds and attracts Zn to its

phenolic group. This complex solution is then placed in an oven at high temperature for 4 h and is converted into  $Zn(OH)_2$ . The zinc hydroxide complex undergoes calcination to form ZnO nanoparticles. This proposed mechanism has been confirmed by other similar reports on the green synthesis of ZnO nanoparticles (33).

The synthesis of the ZnO nanoparticles in aquatic environments also has some problems. One of the main challenges in the application of ZnO-NPs in aqueous media is homodespersion of nanoparticles. This process is difficult due to the tendency of ZnO-NPs to agglomerate. The agglomeration of ZnO nanoparticles changes their size and surface chemistry and affects the interaction between nanomaterials and biological substances. To overcome this problem, we use silica gel, as an amorphous matrix in the green synthesis of ZnO-NPs. Amorphous  $SiO_2$  matrix has uniform particles that can be immobilized, increase the surface area of ZnO-NPs, prepare homodispersed nanoparticles, and prevent agglomeration.

Furthermore, when ZnO-NPs are loaded on silicagel matrix, there would be an interaction between the  $SiO_2$  matrix and Zn-O bond. This interaction decreases Zn-O bonding in nanoparticles and prevents their agglomeration.

The morphology of the biosynthesized ZnO-NPs loaded on silica gel was analyzed by an SEM microscope. The SEM images revealed that the ZnO nanoparticles were spherical with an average diameter of 38 nm (**Fig.1**). The elemental analysis of ZnO/SG nanocomposite was confirmed by EDX, which exhibited remarkable signals for Zn, O and Si (**Fig. 1**).

Furthermore, the structure of ZnO/SG nanocomposites was confirmed by an X-ray diffraction analysis (Fig. 2). The comparison of the observed XRD pattern of ZnO/SG nanocomposites and the XRD pattern of synthesized ZnO-NPs and silica gel matrix show some identical peaks, which confirmed loading ZnO nanoparticles in SiO<sub>2</sub> matrix. This is consistent with the research literature (34). Comparing the observed XRD pattern and the standard ICOD card data indicates that all the peaks are matched with standard ICOD card No. 00-023-1172, indicating that the ZnO-NPs stabilized on silica gel and ZnO-NPs are of hexagonal type.

FT-IR spectrum (Fig. S2, supplementary file) exhibits ZnO-NPs stretching vibration and some possible adherent organic compounds contributing to the stabilization and capping of ZnO nanoparticles.

The effect of silica gel matrix on increasing the surface area was examined using BET analysis (Fig. 3). This analysis provides a precise evaluation of specific surface area for ZnO/SG nanocomposites, compared to unsupported ZnO-NPs, with nitrogen adsorption measured as a function of relative pressure exhibiting type IV isotherms. The result showed that, compared to unsupported ZnO-NPs, the specific surface area increased by  $20.78 \times 10 \text{ m}^2 \cdot \text{g}^{-1}$ , total pore volume enhanced by 0.3586, and the average pore diameter decreased by 13.22 nm. These results lead to the uniform distribution of ZnO-NP nanoparticles inside the SiO<sub>2</sub> pores and are consistent with the observed results in a similar structures (35).

The structure of the biosynthesized ZnO/SG nanocomposite was compared with the chemically synthesized form using SEM analysis (Figure S3, supplementary file). The results show that crystallite size, morphology, and particle size of ZnO-NP in the biosynthesis method are similar to those of the chemical methods. However, the biological methods seem to provide tightly controlled particle size, which is one of their advantages to the chemical methods. One of the specific properties of ZnO nanoparticles is their antibacterial activity against many pathogens (36). Bacterial infections represent a major public health burden because of not only high morbidity and mortality rates but also for increased expenditure on patient management and infection control measures. For example, *Bacillus cereus* and *Salmonella enterica* represent a major cause of food poisoning in various raw or processed food products such as rice, vegetables, meat, and egg. The consumption of food contaminated with these bacteria results in illnesses, including emetic and diarrheal. *Staphylococcus epidermidis*, *Escherichia coli* and *Klebsiella pneumoniae* are established human

pathogens in the hospital environment, inducing a wide range of clinical infections such as pneumonia, meningitis, and toxic shock syndrome. Furthermore, some infections caused by pathogens transmitted from fish or the aquatic environment such as *Edwardsiella tarda* and *Loctococcus garvieae* lead to gastrointestinal or skin diseases in human. For this reason, controlling microbial infections in biological systems and aquatic environments is highly important.

According to the results, it is found out that ZnO/SG nanocomposite is effective antibacterial agents both on Gram-positive and Gram-negative bacteria and fish pathogens (37).

However, the activity mechanism of ZnO nanoparticles against microorganisms is still unknown, and a prevailing hypothesis is that ZnO-NPs spontaneously produce the reactive oxygen species of ROS (including hydroxyl or hydroperoxyl radicals and superoxide ions) and enhance the intracellular oxidative stress in bacteria, which leads to their death (38). Furthermore, some researchers believe that direct or electrostatic interaction between ZnO and cell surfaces can damage DNA and cell membrane (39).

In this research, the main mechanism seems to be the ZnO release from ZnO/SG nanocomposites and the interaction between ZnO and cell surfaces. Furthermore, the reactive surface of the nanomaterials is of great importance in antimicrobial activities because the microorganism can interact with the nanoparticle surface. Therefore, the antibacterial activity of ZnO/SG nanocomposites is much greater than that of ZnO-NPs. On the other hand, an increase in the surface area resulted in the higher coating of silica gel matrix by ZnO and increased the probability of contact between ZnO-NPs and bacteria. Moreover, the stabilization of nanoparticles on SiO<sub>2</sub> prevents the agglomeration of nanoparticles and enhances antibacterial activity.

## 6. Conclusion

In this study, we reported a pro-environmental procedure for the ZnO-NPs synthesis with *Daphne oleoides* extract as a new and native plant extract in Iran. In this regard, it is a great challenge to prepare highly dispersed small ZnO-NPs with acceptable stability and durability. In this study, we used silica gel as a low-cost inert matrix to prepare ZnO/SG nanocomposite, as a highly dispersed nanoparticles structure. The characterization of the nanocomposites structure demonstrates that ZnO-NPs with an average particle size of 38 nm were uniformly dispersed in the silica gel matrix. The BET surface area measurement confirmed that the specific surface area and total pore volume of ZnO/SG nanocomposite

enhanced, compared to unsupported ZnO-NPs. Furthermore, a significant increase was observed in the antibacterial activity of ZnO/SG nanocomposites but not ZnO-NPs, and this structure can be used as a strong antibacterial nanocomposite in biological applications. Accordingly, this procedure can be used as an effective green method for the ZnO/SG nanocomposite synthesis in biological applications.

## References

- Wang P, Lombi E, Zhao F-J, Kopittke PM. Nanotechnology: a new opportunity in plant sciences. *Trends Plant Sci.* 2016;**21**(8):699-712. <https://doi.org/10.1016/j.tplants.2016.04.005>
- Rogers MA. Naturally occurring nanoparticles in food. *Curr Opin Food Sci.* 2016;**7**:14-19. <https://doi.org/10.1016/j.cofs.2015.08.005>
- Ansari SA, Satar R, Jafri MA, Rasool M, Ahmad W, Zaidi SK. Role of nanodiamonds in drug delivery and stem cell therapy. *Iran J Biotechnol.* 2016;**14**(3):130-141. <https://dx.doi.org/DOI:10.15171/ijb.1320>
- Das DK, Sarkar J. Theoretical calculation of atomic and physical properties of some low-dimensional nanomaterials. *Mater Today-Proc.* 2018; **5**(14, Part 2):27982-27988. <https://doi.org/10.1016/j.matpr.2018.10.038>
- Mohammad-Beigi H, Shojaosadati SA, Morshedi D, Mirzazadeh N, Arpanaei A. The effects of organic solvents on the physicochemical properties of human serum albumin nanoparticles. *Iran J Biotechnol.* 2016;**14**(1):45-50. <https://dx.doi.org/10.15171/ijb.1168>
- Falcaro P, Ricco R, Yazdi A, Imaz I, Furukawa S, MasPOCH D, et al. Application of metal and metal oxide nanoparticles@MOFs. *Coord Chem Rev.* 2016;**307**:237-254. <https://doi.org/10.1016/j.ccr.2015.08.002>
- Garcia CV, Shin GH, Kim JT. Metal oxide-based nanocomposites in food packaging: applications, migration, and regulations. *Trends Food Sci Tech.* 2018;**82**:21-31. <https://doi.org/10.1016/j.tifs.2018.09.021>
- Dizaj SM, Lotfipour F, Barzegar-Jalali M, Zarrintan MH, Adibkia K. Antimicrobial activity of the metals and metal oxide nanoparticles. *Mater Sci Eng. C.* 2014;**44**:278-284. <https://doi.org/10.1016/j.msec.2014.08.031>
- Mazaheri N, Naghsh N, Karimi A, Salavati H. In vivo toxicity investigation of magnesium oxide nanoparticles in rat for environmental and biomedical applications. *Iran J Biotechnol.* 2019;**17**(1):1-9. <https://dx.doi.org/10.21859/ijb.1543>
- Mohammadi S, Nikkhal M. TiO<sub>2</sub> nanoparticles as potential promoting agents of fibrillation of  $\alpha$ -synuclein, a parkinson's disease-related protein. *Iran J Biotechnol.* 2017;**15**(2):87-94. <https://dx.doi.org/DOI:10.15171/ijb.1519>
- Fathi Azar Khavarani M, Najafi M, Shakibapour Z, Zaeifi D. Kinetics activity of yersinia intermedia against ZnO nanoparticles either synergism antibiotics by double-disc synergy test method. *Iran J Biotechnol.* 2016;**14**(1):39-44. <https://dx.doi.org/10.15171/ijb.1184>
- Liu J-H, Ma X, Xu Y, Tang H, Yang S-T, Yang Y-F, et al. Low toxicity and accumulation of zinc oxide nanoparticles in mice after 270-day consecutive dietary supplementation. *Toxicol Res.* 2017;**6**(2):134-143. <http://dx.doi.org/10.1039/c6tx00370b>
- Mohd Omar F, Abdul Aziz H, Stoll S. Aggregation and disaggregation of ZnO nanoparticles: influence of pH and adsorption of Suwannee River humic acid. *Sci Total Environ.* 2014;**468**:195-201. <https://doi.org/10.1016/j.scitotenv.2013.08.044>
- Chen Y, Ding H, Sun S. Preparation and characterization of ZnO nanoparticles supported on amorphous SiO<sub>2</sub>. *Nanomaterials.* 2017;**7**(8):217-221. <https://doi.org/10.3390/nano7080217>
- Rashidi L, Vasheghani-Farahani E, Rostami K, Gangi F, Fallahpour M. Mesoporous silica nanoparticles as a nanocarrier for delivery of vitamin C. *Iran J Biotechnol.* 2013;**11**(4):209-213. <https://dx.doi.org/10.5812/ijb.14279>
- Babu KS, Reddy AR, Reddy KV. Controlling the size and optical properties of ZnO nanoparticles by capping with SiO<sub>2</sub>. *Mater Res Bull.* 2014;**49**:537-543. <https://doi.org/10.1016/j.materresbull.2013.09.024>
- Saleh SM. ZnO nanospheres based simple hydrothermal route for photocatalytic degradation of azo dye. *Spectrochim Acta A: Mol Biomol Spectrosc.* 2019;**211**:141-147. <https://doi.org/10.1016/j.saa.2018.11.065>
- Mariya Joseph H, Poornima N. Synthesis and characterization of ZnO nanoparticles. *Mater Today-Proc.* 2019; **9**:7-12. <https://doi.org/10.1016/j.matpr.2019.02.029>
- Nithya K, Kalyanasundharam S. Effect of chemically synthesis compared to biosynthesized ZnO nanoparticles using aqueous extract of *C. halicacabum* and their antibacterial activity. *Open Nano.* 2019;**4**:100024-100036. <https://doi.org/10.1016/j.onano.2018.10.001>
- Kharissov OV, Dias HVR, Kharisov BI, Perez BO, Perez VMJ. The greener synthesis of nanoparticles. *Trends Biotechnol.* 2013;**31**(4):240-8. <https://doi.org/10.1016/j.tibtech.2013.01.003>
- Abdellatif KF, Hamouda RA, El-Ansary MSM. Green nanoparticles engineering on root-knot nematode infecting eggplant plants and their effect on plant DNA modification. *Iran J Biotechnol.* 2016;**14**(4):250-259. <https://dx.doi.org/10.15171/ijb.1309>
- Gour A, Jain NK. Advances in green synthesis of nanoparticles. *Artif Cells Nanomed Biotechnol.* 2019;**47**(1):844-851. <https://doi.org/10.1080/21691401.2019.1577878>
- Dhanmozhi C, Rajeswari V, Sathyajothi S. Green synthesis of zinc oxide nanoparticle using green tea leaf extract for supercapacitor application. *Mater Today-Proc.* 2017;**4**(2, Part A):660-667. <https://doi.org/10.1016/j.matpr.2017.01.070>
- Nava OJ, Soto-Robles CA, Gomez C, Vilchis-Nestor A, Castro-Beltran A, Olivas A, et al. Fruit peel extract mediated green synthesis of zinc oxide nanoparticles. *J Mol Struct.* 2017;**1147**:1-6. <https://doi.org/10.1016/j.molstruc.2017.06.078>
- Sutradhar P, Saha M. Green synthesis of zinc oxide nanoparticles using tomato (*Lycopersicon esculentum*) extract and its photovoltaic application. *J Exp Nanosci.* 2016;**11**(5):314-327. <https://doi.org/10.1080/17458080.2015.1059504>
- Siripireddy B, Mandal BK. Facile green synthesis of zinc oxide nanoparticles by *Eucalyptus globulus* and their photocatalytic and antioxidant activity. *Adv Powder Technol.* 2017;**28**(3):785-797. <https://doi.org/10.1016/j.apt.2016.11.026>
- Sharmila G, Thirumarimurugan M, Muthukumaran C. Green synthesis of ZnO nanoparticles using *Tecoma castanifolia* leaf extract: characterization and evaluation of its antioxidant, bactericidal and anticancer activities. *Microchem J.* 2019;**145**:578-587. <https://doi.org/10.1016/j.microc.2018.11.022>
- Thema FT, Manikandan E, Dhlamini MS, Maaza M. Green

- synthesis of ZnO nanoparticles via *Agathosma betulina* natural extract. *Mater Lett.* 2015;**161**:124-127. <https://doi.org/10.1016/j.matlet.2015.08.052>
29. Balkan IA, Taskın T, Dogan HT, Deniz I, Akaydın G, Yesilada E. A comparative investigation on the in vitro anti-inflammatory, antioxidant and antimicrobial potentials of subextracts from the aerial parts of *Daphne oleoides* Schreb. subsp. *oleoides*. *Ind Crop Prod.* 2017;**95**:695-703. <https://doi.org/10.1016/j.indcrop.2016.11.038>
30. Atkins JW, West K, Kasow KA. Current and future cell therapy standards and guidelines. *Hematol Oncol Clin North Am.* 2019. *In press*, <https://doi.org/10.1016/j.hoc.2019.05.008>
31. Gharagozlou M, Naghibi S. Sensitization of ZnO nanoparticle by vitamin B<sub>12</sub>: Investigation of microstructure, FTIR and optical properties. *Mater Res Bull.* 2016;**84**:71-78. <https://doi.org/10.1016/j.materresbull.2016.07.029>
32. Parveen K, Banse V, Ledwani L. Green synthesis of nanoparticles: Their advantages and disadvantages, Conference: *5th National Conference on Thermophysical Properties* : (NCTP-09) 2016. 020048 p. <https://doi.org/10.1063/1.4945168>
33. Senthilkumar N, Nandhakumar E, Priya P, Soni D, Vimalan M, Vetha Potheher I. Synthesis of ZnO nanoparticles using leaf extract of *Tectona grandis* (L.) and their anti-bacterial, anti-arthritis, anti-oxidant and in vitro cytotoxicity activities. *New J Chem.* 2017;**41**(18):10347-56. <https://doi.org/10.1039/C7NJ02664A>
34. Bharati R, Suresh S. Biosynthesis of ZnO/SiO<sub>2</sub> nanocatalyst with palash leaves' powder for treatment of petroleum refinery effluent. *Resource-Efficient Technologies.* 2017;**3**(4):528-41. <https://doi.org/10.1016/j.reffit.2017.08.004>
35. Bahrami K, Karami Z. Core/shell structured ZnO@SiO<sub>2</sub>-TTIP composite nanoparticles as an effective catalyst for the synthesis of 2-substituted benzimidazoles and benzothiazoles. *J. Exp. Nanosci.* 2018;**13**(1):272-283. <https://doi.org/10.1080/17458080.2018.1542511>
36. Siddiqi KS, Ur Rahman A, Tajuddin, Husen A. Properties of zinc oxide nanoparticles and their activity against microbes. *Nanoscale Res Lett.* 2018;**13**(1):141-154. <https://doi.org/10.1186/s11671-018-2532-3>
37. Gunalan S, Sivraj R, Rajendran V. Green synthesized ZnO nanoparticles against bacterial and fungal pathogens. *Prog Nat Sci: Mater Int.* 2012;**22**(6):693-700. <https://doi.org/10.1016/j.pnsc.2012.11.015>
38. Tiwari V, Mishra N, Gadani K, Solanki PS, Shah NA, Tiwari M. Mechanism of anti-bacterial activity of zinc oxide nanoparticle against carbapenem-resistant *Acinetobacter baumannii*. *Front Microbiol.* 2018;**9**:1218-1229. <https://doi.org/10.3389/fmicb.2018.01218>
39. Xie Y, He Y, Irwin PL, Jin T, Shi X. Antibacterial activity and mechanism of action of zinc oxide nanoparticles against *Campylobacter jejuni*. *Appl Environ Microbiol.* 2011;**77**(7):2325-3231. <https://doi.org/10.1128/AEM.02149-10>